ISSN 2072-5981
doi: 10.26907/mrsej

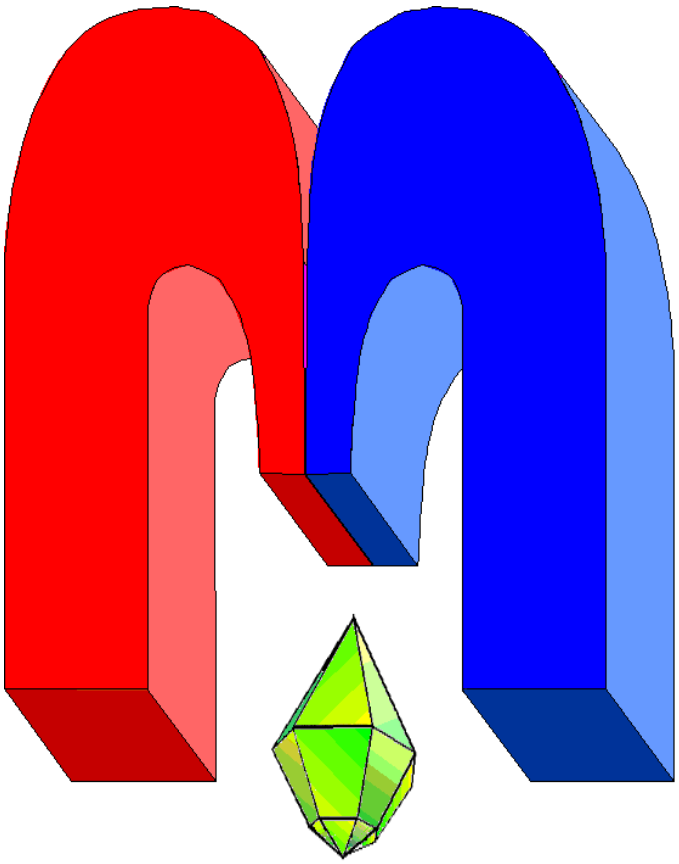

Magnetic Resonance in Solids

Electronic Journal

Volume ***21***
Special Issue ***4***
Paper No ***19411***
1-6 pages
2019
doi: **10.26907/mrsej-19411**

http://mrsej.kpfu.ru
http://mrsej.ksu.ru

Established and published by Kazan University
Endorsed by International Society of Magnetic Resonance (ISMAR)
Registered by Russian Federation Committee on Press (#015140), August 2, 1996
First Issue appeared on July 25, 1997

"***Magnetic Resonance in Solids. Electronic Journal***" (**MRS*ej***) is a peer-reviewed, all electronic journal, publishing articles which meet the highest standards of scientific quality in the field of basic research of a magnetic resonance in solids and related phenomena.

Indexed and abstracted by
Web of Science (*ESCI*, Clarivate Analytics, from 2015), *Scopus* (Elsevier, from 2012), *RusIndexSC* (*eLibrary*, from 2006), *Google Scholar*, *DOAJ*, *ROAD*, *CyberLeninka* (from 2006), *SCImago Journal & Country Rank*, etc.

* In Kazan University the Electron Paramagnetic Resonance (EPR) was discovered by Zavoisky E.K. in 1944.

Short cite this: *Magn. Reson. Solids* **21**, 19411 (2019) doi: 10.26907/mrsej-19411

EPR evidence of surface paramagnetic defects formation due to annealing of LaF_3 nanoparticles

R.M. Rakhmatullin*, M.S. Pudovkin**, V.V. Semashko

Kazan Federal University, Kremlevskaya 18, Kazan 420008, Russia

**E-mail: rafail.rakhmatullin@kpfu.ru*

***E-mail: jaz7778@list.ru*

(Received May 27, 2019; accepted May 28, 2019; published June 6, 2019)

An EPR technique and optical measurements have been applied to study LaF_3 nanoparticles doped with 7% of Pr^{3+} ions. It has been found that vacuum annealing of the studied samples leads to the appearance of paramagnetic defects with g-factor close to the value which is typical for the electron trapped in a fluorine vacancy. The concentration of paramagnetic defects was reduced after fluorination of initial nanoparticles. The possible origin of surface defects due to vacuum annealing is discussed. The results of the study can help to improve the performance of fluoride nanoparticles for biomedical applications.

PACS: 76.30.-v, 76.30.Kg.

Keywords: fluoride nanoparticles, EPR, surface paramagnetic defect, luminescence.

This article is devoted to Professor B.Z. Malkin, whose significant contribution in the study of rare earth-doped fluoride crystals helped us in our researches

1. Introduction

Fluoride nanoparticles are promising materials for applications in such areas as catalysis, optoelectonics and biomedicine [1–7]. For biomedical applications of particular interest are luminescent nanoparticles [8], which, due to their optical properties, may be used for optical and magnetic imaging applications both in vitro and in vivo [9]. Rare earth doped fluorides have been considered as an excellent luminescent materials, because they normally possess a high refractive index and low phonon energy, excellent photostability, long luminescent lifetimes (micro-to milliseconds), sharp emission bands, high chemical stability, and lack of photobleaching [2,3,10–13]. Among a big variety of luminescent rare earth doped fluoride nanomaterials, Pr^{3+} doped fluoride nanoparticles are considered very promising for some mentioned above applications especially in luminescent thermometry. Indeed, it has been reported that because of thermally coupled $^3P_1$ to $^3P_0$ electronic states of Pr^{3+} ions Pr^{3+} doped nanomaterials [14] demonstrate high temperature sensitivity of luminescent signal into a broad temperature range including physiological temperature range. The emission spectrum of Pr^{3+} ions in some host matrices overlaps with photosensitizers such as acridine ($C_{13}H_9N$) and cyanine which are highly relevant in "hybrid" radiotherapy – photodynamic therapy (PDT) [15]. Specifically Pr^{3+}:LaF_3 ($C_{Pr} = 7\%$) nanoparticles demonstrate excellent luminescent properties and high absolute temperature sensitivity ($0.01\%K^{-1}$) [14]. The synthesis procedures of these nanoparticles are relatively simple and cost effective in comparison to some counterparts [14, 16]. However, fluoride nanomaterials can contain a large number of surface defects that degrade luminescent characteristic of these nanoparticles. For example in some cases the undesirable oxyfluoride formation takes place [3]. In order to understand the fundamental properties of nanomaterials and improve the synthesis techniques the nanomaterials must be characterized by different methods including electron paramagnetic resonance (EPR).

The purpose of this work was to apply optical and EPR spectroscopic techniques to study the effects of fluorination and annealing on the Pr^{3+}:LaF_3 ($C_{Pr} = 7\%$) nanoparticles. This study can help to improve the efficiency of the rare earth doped fluoride nanoparticles.

2. Materials and methods

Pr^{3+}:LaF_3 ($C_{Pr} = 7\%$) nanoparticles (molar ratio of Pr^{3+} and La^{3+} ions is 7:93) were synthesized via co-precipitation method using common chemical reaction for rare earth elements described in [14]. For example, in order to synthesize Pr^{3+}:LaF_3 ($C_{Pr} = 7\%$) nanoparticles, 0.188 g of Pr_2O_3 and 2.500 g and La_2O_3 were added to 70 mL of 10% nitric acid in a glass beaker. The mixture was heated to 50°C and stirred for 45 min then a transparent light-green solution appeared. The pH of the solution was 1. Then the mixture was filtered, poured in a polypropylene glass and placed in an ultrasonic cleaner (model UD100SH-2LQ, ultrasonic power 100W) and solution of 1.045 g, 6.270 g of NaF into 160 mL of distillated water was added. The pH was adjusted to 4 by adding 25% solution of ammonium hydrate. The mixture was stirring for 10 minutes under the ultrasonic treatment. The precipitate was purified with distillated water by centrifugation (12000 rpm, centrifugation time was 15 min) 8 times. Then nanoparticles were dried on air at room temperature in the dust-free box. For this study we prepared 3 types of samples: 1) the initial or as prepared nanoparticles Pr^{3+}:LaF_3 ($C_{Pr} = 7\%$), 2) nanoparticles Pr^{3+}:LaF_3 ($C_{Pr} = 7\%$) subjected to fluorination, 3) nanoparticles Pr^{3+}:LaF_3 ($C_{Pr} = 7\%$) annealed in vacuum chamber at 300°C for 3 hours.

Fluorination procedure was following. The 50 ml solution containing 0.8 g of Pr^{3+}:LaF_3 ($C_{Pr} = 7\%$) nanoparticles was placed on the magnetic stirring. Then, 50 ml of 40 g/l NaF solution was added dropwize. The obtained mixture was stirred for 2 h at room temperature. Then, the nanoparticles were purified with distillated water by centrifugation. The structure of the material was characterized by X-ray diffraction method with Shimadzu XRD-7000S X-ray diffractometer. Analysis of samples was carried out in a transmission electron microscope Hitachi HT7700 Exalens. Sample preparation: 10 microliters of the suspension was placed on a formvar/carbon lacey 3mm copper grid, drying was performed at room temperature. After drying, grid was placed in a transmission electron microscope using special holder for microanalysis. Analysis was held at an accelerating voltage of 100 kV in TEM mode, the elemental analysis was carried out in STEM mode, at the same parameters using Oxford Instruments X-Max^{TM} 80 T detector. EPR measurements of the studied samples were made using a Bruker ESP 300 cw spectrometer working in the X-band ($\sim$ 9.42 GHz) with field modulation of 100 kHz. The temperature of the samples was controlled with a continuous-flow helium cryostat (Oxford Instruments ESR 900).

3. Results and discussion

Transmission electron microscopy (TEM) data indicate that as prepared Pr^{3+}:LaF_3 ($C_{Pr} = 7\%$) samples consist of nearly monodisperse nanoparticles. The shape of these nanoparticles is not perfectly spherical (Fig. 1). An average nanoparticles diameter is 19 nm. According to the X-ray diffraction data (Fig. 2) the as prepared Pr^{3+}:LaF_3 ($C_{Pr} = 7\%$) nanoparticles were hexagonal structured nanocrystals. Sharp peaks of the patterns (full width at half maximum (FWHM) of (111) peak is 0.512 ± 0.003 degrees) confirm good crystallinity of the nanoparticles. The lattice parameters for as prepared Pr^{3+}:LaF_3 ($C_{Pr} = 7\%$) nanoparticles are $a = 0.7123(2)$ nm and $c = 0.7297(4)$ nm. These values are different from the lattice parameters for LaF_3 (JCPDS-32-0483) $a = 0.7718$ nm and $c = 0.7352$ nm because of the crystal lattice distortion. The radius of Pr^{3+} (0.105 nm) is smaller than that of La^{3+} (0.113 nm) due to the lanthanide contraction,

so the cell volume of Pr^{3+}:LaF_3 reduces with more Pr^{3+} replacing La^{3+}. The average size of as prepared Pr^{3+}:LaF_3 ($C_{Pr} = 7\%$) nanoparticles was calculated using Debye-Scherrer formula:

$$D = \frac{K\lambda}{B_{hkl} \cos A}, \tag{1}$$

where D is the mean size of a nanoparticle, K is the shape factor (we used $K = 0.9$), λ is the X-ray wavelength (0.15418 nm), B_{hkl} (111) is the line broadening at half the maximum intensity (FWHM) in radians, A is the Bragg angle (in degrees). The D values of all the nanoparticles are around 12 nm, which is in good accordance with HR TEM data. It can be concluded that the peak broadening of the XRD spectra is mainly related to the nanoscale dimensionality of the crystalline particles. The EDX spectroscopy indicates that the as prepared Pr^{3+}:LaF_3 ($C_{Pr} = 7\%$) nanoparticles contain Pr, La, and F. The room-temperature luminescence spectrum of as prepared and vacuum annealed Pr^{3+}:LaF_3 ($C_{Pr} = 7\%$) nanoparticles excited by the pulse laser beam at 444 nm is presented in Fig. 3. The luminescent spectra of both samples have the emissions bands at about 487, 523, 537, 580, 601, and 672 nm which are interpreted as the result of the transition from the ^3P_j ($j = 0, 1, 2$) excited states to $^3H_4$, $^3H_5$, $^3H_5$, $^3H_6$ and $^3F_4$ states of Pr^{3+} ions, respectively. The emissions bands corresponding to impurities or any unidentified bands are not found. However, in case of annealed nanoparticles the broad peak of fluorescent background was clearly observed. Moreover, the emissions bands were notably weaker in comparison to the emissions bands of Pr^{3+}:LaF_3 ($C_{Pr} = 7\%$) nanoparticles. It should be added

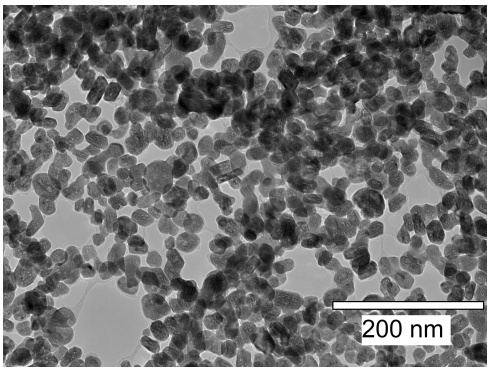

Figure 1. Transition electron microscopy image of the as prepared Pr^{3+}:LaF_3 ($C_{Pr} = 7\%$) nanoparticles.

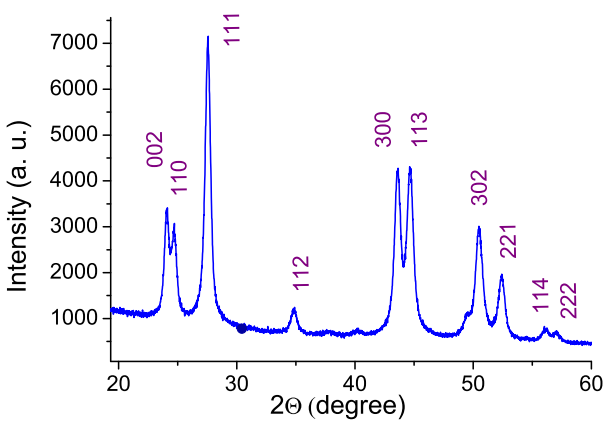

Figure 2. X-ray diffraction pattern of the Pr^{3+}:LaF_3 ($C_{Pr} = 7\%$) nanoparticles. The (hkl) indices of the LaF_3 structure are labeled.

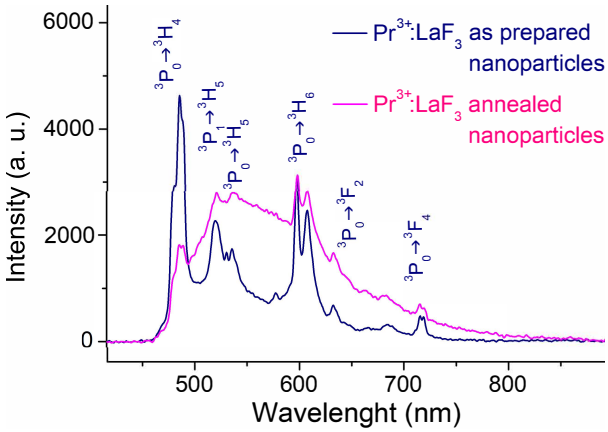

Figure 3. Luminescence spectra of as prepared (initial) Pr^{3+}:LaF_3 ($C_{Pr} = 7\%$) nanoparticles and Pr^{3+}:LaF_3 ($C_{Pr} = 7\%$) nanoparticles annealed at 300°C, normalized at $\lambda = 601$ nm ($\lambda_{ex} = 444$ nm, $T = 24$°C).

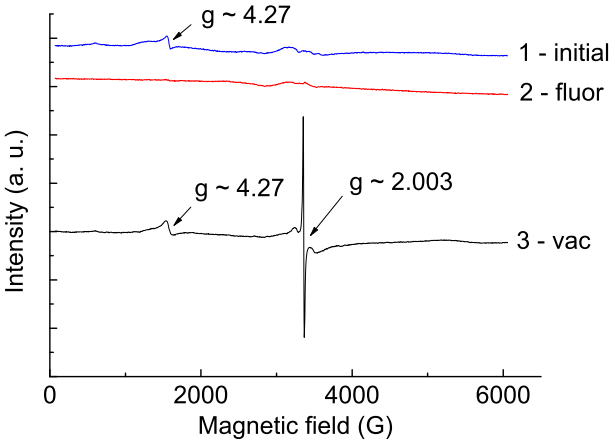

Figure 4. EPR spectra of Pr^{3+}:LaF_3 ($C_{Pr} = 7\%$) nanoparticles at low temperature (15 K). 1. Initial (as prepared) nanoparticles. 2. Fluorinated nanoparticles. 3. Vacuum annealed nanoparticles. The measurement conditions were the same for all three samples.

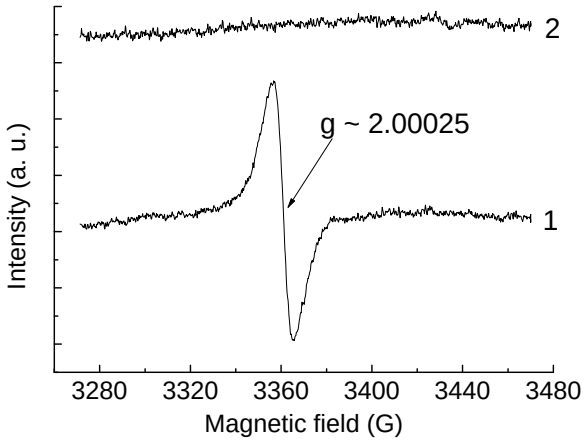

Figure 5. EPR spectra of Pr^{3+}:LaF_3 ($C_{Pr} = 7\%$) at the room temperature. 1. Vacuum-annealed Pr^{3+}:LaF_3 ($C_{Pr} = 7\%$). 2. Fluorinated nanoparticles. The measurement conditions were the same for both cases.

that after annealing the Pr^{3+}:LaF_3 ($C_{Pr} = 7\%$) powder became brown. It may be suggested that as a result of annealing the formation of oxyfluoride takes place. In such matrix the processes of luminescence quenching are more effective. In addition the fluorescent background can be attributed to the energy transfer from rare earth ion to oxygen.

EPR spectra of Pr^{3+}:LaF_3 ($C_{Pr} = 7\%$) nanoparticles are shown in Fig. 4 and Fig. 5. It is known that Pr^{3+} is a non-Kramers ion and the observation of EPR of this type of ions is quite difficult with the usual EPR techniques. Besides the high concentration of Pr^{3+} ions leads to broadening of the lines due to dipolar interactions. So we did not detect the EPR lines that could be assigned to Pr^{3+}. It should be noted that EPR of LaF_3 nanocrystals containing considerably less amount of Pr^{3+} ions ($C_{Pr} = 1\%$) was recently published [17]. Similar to results of our measurements authors of ref. [17] did not detect the EPR absorption lines due to Pr^{3+} ions. The EPR spectra of initial (as prepared) as well as vacuum annealed nanoparticles measured at 15 K have the line with $g \sim 4.27$ that is typical for Fe^{3+} ions in glassy or disordered solids [18]. This line is also observed earlier in CeO_2 nanoparticles containing a small amount of Fe^{3+} [19]. The concentration of this impurity is rather low (less than 10 ppm) and the optical techniques as well as EDX techniques used for the elemental composition analysis of nanoparticles could not detect it. The fluorination of initial (as prepared) nanoparticles leads to disappearance of this line. The possible reason for this could be the change of the valence state of the iron due to fluorination. The rather intensive line at $g \sim 2.003$ is observed in the vacuum annealed sample. This line is also observed at the room temperature as can be seen in Fig. 5 in comparison to the fluorinated sample. The origin of this line is not quite clear but we supposed the formation of the paramagnetic center that consists of an electron trapped in the fluorine vacancy. Such center may be related to the formation of oxyfluoride as has been suggested from luminescence measurements.

4. Summary

The comparative study of as prepared, fluorinated and vacuum annealed Pr^{3+}:LaF_3 ($C_{Pr} = 7\%$) nanoparticles has been carried out using EPR and optical spectroscopy. The optical measurements revealed that emissions bands of vacuum annealed Pr^{3+}:LaF_3 ($C_{Pr} = 7\%$) nanoparticles

were notably weaker in comparison to the emissions bands of as prepared Pr^{3+}:LaF_3 ($C_{Pr} = 7\%$) nanoparticles. We supposed that vacuum annealing leads to the formation of the oxyfluoride at the surface of the studied nanoparticles. EPR measurements showed that the fluorination of Pr^{3+}:LaF_3 ($C_{Pr} = 7\%$) nanoparticles leads to the reduction of EPR lines related to the trace impurity as compared to as prepared Pr^{3+}:LaF_3 ($C_{Pr} = 7\%$) nanoparticles. In the vacuum annealed sample the EPR line at $g \sim 2.003$ is observed that was assigned to the paramagnetic center of an electron trapped in the fluorine vacancy.

Acknowledgments

This EPR study and characterization of the nanoparticles works were funded by the subsidy allocated to Kazan Federal University for the state assignment in the sphere of scientific activities [No. 3.1156.2017/4.6, No. 3.5835.2017/6.7]. The optical spectroscopy study was supported by the research grant of Kazan Federal University. Microscopy studies were carried out at the Interdisciplinary Center of Analytical Microscopy of Kazan Federal University. The EPR measurements were done using the equipment of the Federal Center of Shared Equipment of Kazan Federal University. The authors are grateful to A. Kiyamov for the help with XRD measurements and A. Rodionov for the help with EPR measurements.

References

1. Yin X., Utetiwabo W., Sun S., Lian Y., Chen R., Yang W. *J. Catalysis* **374**, 43 (2019)
2. Sobolew B.P. *The Rare Earth Trifluorides*, Institut d'Estudis Catalans, Barcelona (2000)
3. Fedorov P.P., Luginina A.A., Kuznetsov S.V., Osiko V.V. *J. Fluorine Chem.* **132**, 1092 (2011)
4. Mayakova M.N., Voronov V.V., Iskhakova L.D., Kuznetsov S.V., Fedorov P.P. *J. Fluorine Chem.* **187**, 33 (2011)
5. Liu C., Hou Y., Gao M. *Adv. Mater.* **26**, 6922 (2014)
6. Pudovkin M.S., Zelenikhin P.V., Krasheninnikova A.O., Korableva S.L., Nizamutdinov A.S., Alakshin E.M., Semashko V.V., Safiullin R.A., Kadirov M.K. *Opt. Spectrosc.* **121**, 590 (2016)
7. Semashko V.V., Pudovkin M.S., Cefalas A.C., Zelenikhin P.V., Gavriil V.E., Nizamutdinov A.S., Kollia Z., Ferraro A., Sarantopoulou E. *Nanoscale Res. Lett.* **13**, 1 (2018)
8. Chatterjee D.K., Rufaihah A.J., Zhang Y. *Biomaterials* **29**, 937 (2008)
9. Chen G., Ohulchanskyy T.Y., Law W.C., Ågren H., Prasad P.N. *Nanoscale* **3**, 2003 (2011)
10. Kaminskii A.A. *Laser Crystals: Their Physics and Properties*, Springer (2013)
11. Malkin B.Z. *Crystal Field and Electron-Phonon Interaction in Rare-Earth Ionic Paramagnets*, in *Modern Problems in Condensed Matter Sciences*, Elsevier Science Publishers B. V. (1987)
12. Pudovkin M.S., Koryakovtseva D.A., Lukinova E.V., Korableva S.L., Khusnutdinova R.S., Kiiamov A.G., Nizamutdinov A.S., Semashko V.V. *J. Nanomater.* 7549325 (2019)
13. Yan R.X., Li Y.D. *Adv. Functional Mater.* **15**, 763 (2005)
14. Pudovkin M.S., Morozov O.A., Pavlov V.V., Korableva S.L., Lukinova E.V., Osin Y.N., Evtugyn V.G., Safiullin R.A., Semashko V.V. *J. Nanomater.* 3108586 (2017)

15. Pudovkin M.S., Zelenikhin P.V., Shtyreva V., Morozov O.A., Koryakovtseva D.A., Pavlov V.V., Osin Y.N., Evtugyn V.G., Akhmadeev A.A., Nizamutdinov A.S., Semashko V.V. *J. Nanotechnol.* 8516498 (2018)

16. Alakshin E.M., Klochkov A.V., Kondratyeva E.I., Korableva S.L., Kiiamov A.G., Nuzhina D.S., Stanislavovas A.A., Tagirov M.S., Zakharov M.Y., Kodjikian S. *J. Nanomater.* 7148307 (2016)

17. Talik E., Zajdel P., Guzik A., Skrzypek D., Lipinska L., Michalska M. *J. Alloys Compd.* **616**, 556 (2014)

18. Klyava Y. *Electron Paramagnetic Resonance Spectroscopy of Disordered Solids*, Riga, USSR (1988) (*in Russian*)

19. Rakhmatullin R.M., Pavlov V.V., Semashko V.V. *Phys. Stat. Sol. B* **253**, 499 (2016)